atmosphere

MDPI

Article

Cadmium and Cadmium/BDE (47 or 209) Exposure Affect Mitochondrial Function, DNA Damage/Repair Mechanisms and Barrier Integrity in Airway Epithelial Cells

Giusy Daniela Albano [1,2], Anna Bonanno [1,2], Angela Marina Montalbano [1,2], Caterina Di Sano [1,2], Giulia Anzalone [1], Rosalia Gagliardo [1,2], Silvia Ruggieri [1] and Mirella Profita [1,2,*]

[1] Institute for Biomedical Research and Innovation (IRIB), National Research Council of Italy (CNR), 90146 Palermo, Italy; giusydaniela.albano@irib.cnr.it (G.D.A.); anna.bonanno@irib.cnr.it (A.B.); angelamarina.montalbano@irib.cnr.it (A.M.M.); caterina.disano@irib.cnr.it (C.D.S.); giulia.anzalone@irib.cnr.it (G.A.); rosaliapaola.gagliardo@irib.cnr.it (R.G.); silvia.ruggieri@irib.cnr.it (S.R.)
[2] Institute of Translational Pharmacology, National Research Council of Italy (CNR), 00133 Rome, Italy
* Correspondence: mirella.profita@irib.cnr.it

Abstract: Heavy metals and Brominated diphenyl ether flame-retardants (BDEs) often coexist in the environment and are capable of inducing injury, cytotoxicity or genotoxicity in human epithelial cells of the lung. We studied the effects of single Cadmium chloride ($CdCl_2$) or $CdCl_2$/BDE (47 or 209) mixtures in airway epithelial cells, using A549 cell line cultured at submerged conditions and air–liquid interface (ALI) (an in vitro model described as physiologically relevant in vivo-like). We evaluated cell viability, oxidative stress, apoptosis, DNA damage/repair (Comet assay, γH2AX phosphorylation ser139), mitochondrial redox balance (NOX-4, Nrf2 and TFAM) and cell barrier integrity (TEER, ZO-1, Claudin-1, E-cadherin-1) in A549 cells exposed to $CdCl_2$ (1 nM to 10 μM), or to $CdCl_2$ (100 nM)/BDEs (47 or 209) (100 nM). $CdCl_2$ (10 μM) reduced cell viability and increased apoptosis. $CdCl_2$ (100 nM) significantly affected DNA-damage/repair (Olive Tail length production), γH2AX phosphorylation and oxidative stress (ROS/JC-1 production) in submerged cell cultures. $CdCl_2$ (100 nM) decreased viability, TEER, ZO-1, Claudin-1 and E-cadherin-1 mRNA expression, and Nrf2 and TFAM while increased NOX-4, in ALI culture of cells. In both cell culture approaches, the cells stimulated with Cadmium/BDEs mixtures did not show a significant increase in the effects observed in the cells treated with $CdCl_2$ alone. $CdCl_2$ inhalation might exert cytotoxicity and genotoxicity, playing a pivotal role in the uncontrolled oxidative stress, damaging DNA and gene expression in airway epithelial cells. No additional or synergistic adverse effects of $CdCl_2$/BDEs mixture were observed in comparison to $CdCl_2$ alone in lung epithelium.

Keywords: apoptosis; DNA damage/DNA repair; oxidative stress; mitophagy; polybrominated di-phenyl ethers; cadmium

Citation: Albano, G.D.; Bonanno, A.; Montalbano, A.M.; Di Sano, C.; Anzalone, G.; Gagliardo, R.; Ruggieri, S.; Profita, M. Cadmium and Cadmium/BDE (47 or 209) Exposure Affect Mitochondrial Function, DNA Damage/Repair Mechanisms and Barrier Integrity in Airway Epithelial Cells. *Atmosphere* **2022**, *13*, 201. https://doi.org/10.3390/atmos13020201

Academic Editors: Haider A. Khwaja, Azhar Siddique and Mirza M. Hussain

Received: 22 December 2021
Accepted: 25 January 2022
Published: 26 January 2022

1. Introduction

Heavy metals such as cadmium (Cd) and the flame retardant known as brominated diphenyl ethers (BDEs) are toxic air pollutants ranked on the Priority List of Hazardous Substances [1] (WHO Regional Office for Europe, 2015; 2019 Substance Priority List). Heavy metals are released into the environment after the burning of coal, diesel fuel, gasoline and other fossil fuels or to the incineration of municipal waste and to the polluting metal alloy and electroplating facilities. Further, they are added to various materials such as electronic equipment, plastics, carpet liners and textiles [2,3]. Cd and BDEs coexisted in dust surface [4], sediment from river [5] and even in organisms [6]. The coexistence of Cd and BDE in the environment and biological systems poses a substantial risk to human health, but their potential joint toxicities remain so far elusive [7]. It was observed that Cd and BDEs are toxicants that cause pulmonary dysfunctions, lung cancer and chronic

obstructive pulmonary disease (COPD) [2,8]. The pollutant mixtures represent more real environmental conditions, and to study their combined toxicity is a more accurate manner to describe the effect of environmental contamination on human health.

Airway epithelium provides a biological barrier and prevents exogenous substances from entering airway mucosa [9]. Indeed, it represents the first line of defense against potential pathogens or noxious agents, promoting oxidative stress, activation of inflammatory cells, the release of inflammatory mediators such as reactive oxygen species (ROS) and cytokines in epithelial cells [10,11]. The epithelium is a monolayer of polarized epithelial cells maintained by the formation of tight (as zonula occludens (ZO)-1 and Claudins) and adherent junctions (as the transmembrane protein E-cadherin), involved in barrier functions and integrity [12,13]. Pollutants induce pulmonary toxicity, promoting a proinflammatory response that disturbs tissue homeostasis via multiple mechanisms, including apoptosis, oxidative stress, DNA damage/repair mechanisms and DNA demethylation disrupting E-cadherin-mediated cell adhesion in lung cells [10,14,15].

Mitochondria are critically implicated in reactive oxygen species (ROS)-dependent lung diseases, such as lung fibrosis, asbestos, chronic airway diseases and lung cancer [16]. Pathological conditions enhanced oxidative stress-inducing endogenous ROS as a product of the functional electron transfer chain in the mitochondria [17]. Mitochondria are the primary source of ROS in the lung and play a key role in the pathogenesis of several chronic lung disorders [18]. Inhibition of NADPH oxidase 4 (NOX-4) expression increased the transcription factor A mitochondrial (TFAM), ensuring mitochondrial DNA replication leading to stimulation of mitochondrial biogenesis [19]. Recent studies demonstrated an increase in NOX-4 activity associated with deficient nuclear factor erythroid 2–related factor 2 (Nrf2) driven cytoprotective responses characterizes this redox imbalance [20]. Nrf2 is an oxidative stress-sensitive transcription factor with a key role in mitochondrial function regulations [21]. Oxidative stress affects mitochondria, which leads to the consequent loss of mitochondrial function and induces the collapse of the electrochemical gradient, which makes the cell more susceptible to damage mediated by ROS [22]. In vitro/ex vivo studies performed with epithelial cells of human lungs, it was observed that BDEs (100 nM) could promote cytotoxic and genotoxic effects [23], inducing inflammatory response and loss of barrier integrity [10].

The aim of the present study is to verify whether Cd exposure of airway human epithelial cells shows additional or synergistic adverse effects in the presence of flame retardants (BDE-47 and -209). Accordingly, we studied the action of Cd chloride ($CdCl_2$) alone or in combination with BDEs in cell functions affected by BDEs as previously described [10,23]. We described the effect of $CdCl_2$ and $CdCl_2$/BDE mixtures in an "in vitro" model of A549 cell line obtained using: (1) submerged cell culture to study cell viability, oxidative stress, apoptosis and DNA damage in epithelial cells cultured in monolayer and (2) 3D ALI cell culture to evaluate cell viability, oxidative stress (NOX-4), redox balance (NOX-4, Nrf2 and TFAM) and barrier integrity (TEER, and ZO-1, Claudin-1 and E-cadherin mRNA expression) in stratified epithelial cells.

2. Materials and Methods

2.1. Chemicals and Solutions

Cadmium chloride ($CdCl_2$) was purchased from Sigma Aldrich (cod. 202908), BDE-47 [2,4,20,40-Tetrabromodiphenyl Ether] (CAS 5436-43-1, 100% purity), and BDE-209 (Decabromodiphenyl ether) (CAS 1163-19-5) from ChemService (West Chester, PA, USA). Stock solutions of $CdCl_2$ (100 mM) were dissolved in distilled water, BD- 47 (25 mM) and BDE-209 (2.5 mM) were prepared in dimethyl sulfoxide (DMSO) purchased from Sigma Aldrich (Milan, Italy). The final dilution of each concentration of BDEs did not exceed 0.05% of DMSO. Human alveolar adenocarcinoma cell line A549 was purchased from American Type Culture Collection (ATCC; Rockville, MD). For cell culture, DMEM (Dulbecco's Modified Eagle's Medium High Glucose with sodium pyruvate, without L-Glutamine-COD. ECB7501L), fetal bovine serum (FBS), non-essential amino acids (MEM), L-glutamine, gen-

tamicin and fungizone were purchased from Euroclone (Milan, Italy). Then, 12-well Transwell inserts Costar 3460 (0.4-µm pore size) were purchased from Corning (New York, NY, USA). Collagen from calf skin (C8919) was purchased from Sigma-Aldrich (Milan, Italy).

2.2. A549 Cell Cultures and Exposure

The human lung adenocarcinoma cell line (A549) was cultured as an adherent monolayer in DMEM supplemented with 10% FBS, 1% MEM, 2 mM L-glutamine and gentamicin 250 µg/mL. For submerged exposures, A549 cells were seeded into standard six-well culture plates at a density of 1 × 105 cells per well and allowed to proliferate to reach 70–80% of confluence. Before exposure to contaminants, cells were starved for 24 h with culture medium FBS free. A549 cells were stimulated with a range of concentrations (0, 1 nM, 10 nM, 100 nM, 1 microM and 10 microM) as previously described in in vitro models of epithelial cells [24,25]. Furthermore, the cells were stimulated with single $CdCl_2$ (100 nM) or $CdCl_2$ (100 nM)/BDEs (47 or 209) (100 nM) mixtures. The single effect of BDEs on the measurements of this study was previously described [10,23]. A549 cells were stimulated for 4 h (to detect ROS and JC1 by cytofluorimetry) or 72 h for viability (MTS), apoptosis (by cytofluorimetry), and DNA damage (Comet assay). For air–liquid interface (ALI) culture, an aliquot of A549 cells (1 × 105) was seeded on 12-well collagen-coated Transwell inserts and grown in DMEM supplemented with 10% FBS, 1% MEM, 2 mM L-glutamine and gentamicin 250 µg/mL, to allow the attachment in the transwell. When A549 reached 90% of confluence (day 0), apical medium was removed and cells were cultured at ALI for 5 days, as previously described [10,26]. A fresh medium was provided every 48 h for 5 days (50 µL in the apical chamber and 1.0 mL in the basal chamber) as previously described [26] to simulate a thin layer of air–liquid in the apical chamber of ALI culture.

Trans-epithelial electrical resistance (TEER) was assessed before and after stimulation to evaluate the integrity of the epithelial layers in ALI culture and to measure the integrity of TJ dynamics, as previously described [10,27] using an EVOM2 Voltohmmeter (World Precision Instruments, Sarasota, USA). ALI were stimulated with $CdCl_2$ (0, 1, 10, 100 nM, 1 and 10 µM) for dose response or with $CdCl_2$ (100 nM) and $CdCl_2$ (100 nM)/BDEs (47 and −209) (100 nM) mixtures for 72 h to detect viability (MTS), TEER, protein expression by Western blot, and mRNA expression. The apical surface of ALI culture was washed with 0.5 mL PBS, then the membranes of transwell inserts (0.4-mm pore size) were cut out and processed for protein extraction and RNA isolation, as described below.

2.3. Cell Proliferation Assay

MTS assay for cell viability was assessed in submerged and ALI experimental conditions. The cells in submerged conditions were plated at a density of 1 × 103 cells per wells in a 96-well plate in 200 µL DMEM 10% FBS and stimulated for 72 h with $CdCl_2$ and BDEs (−47 and −209) alone for dose response or combined in mixtures. For ALI culture, the viability was evaluated in cells seeded on 12-well collagen-coated Transwell inserts, as previously described with minor modification [10,15] and stimulated with CdCl2 for dose response and with BDEs mixtures. Cell viability was determined in vitro by 3-(4,5-dimethylthiazol-2-yl)-5-(3-carboxymethoxyphenyl)-2-(4-sulfophenyl)-2H-tetrazolium MTS assay, using the Cell Titer 96® Aqueous One Solution Cell Proliferation Assay kit (Promega, Madison, WI, USA), according to the manufacturer's instruction. The MTS is reduced by cells into a formazan product, soluble in tissue culture medium, quantified using Wallac 1420 Victor2 multilabel counter (PerkinElmer Life Sciences, Turku, Finland) at 450 nm. The absorbance is directly proportional to the number of living cells in culture; results are expressed as % of baseline. Untreated controls were incubated in the same plates and under the same conditions [10,15].

2.4. Detection of Intracellular ROS

The reactive oxygen species (ROS) were detected in A549 stimulated for 4 h with $CdCl_2$ (0, 1, 10, 100 nM, 1 and 10 µM) for dose response or with $CdCl_2$ (100 nM) and

$CdCl_2$ (100 nM)/BDEs (47 and −209) (100 nM) mixtures. A549 cells cultured in submerged conditions were trypsinized, washed in PBS and incubated in PBS with DCFH-DA (2, 7-dichloro-difluorescein diacetate, Molecular Probes, OR, USA) 1 µM in PBS for 10 min (in the dark at room temperature). The intracellular ROS generation was evaluated by flow cytometry analyses using a FACSCaliburTM flow cytometer (Becton Dickinson, Mountain View, CA, USA) as previously described [23].

2.5. Detection of JC-1 Mitochondrial Membrane Potential to Assess Mitochondrial Function

JC-1 was detected in A549 stimulated for 4 h $CdCl_2$ (0, 1, 10, 100 nM, 1 and 10 µM) for dose response or with $CdCl_2$ (100 nM) and $CdCl_2$ (100 nM)/BDEs (47 and −209) (100 nM) mixtures. The mitochondrial function was assessed by membrane potential analysis using MitoProbe JC-1 Assay kit M34152 (Molecular Probes, Eugene, OR, USA), a lipophilic cationic dye as previously described [28]. JC-1 localizes to the mitochondrial inner membrane forming either aggregates (reflecting a high membrane potential as indicated by red fluorescence) or monomers (reflecting a low membrane potential and fluorescing green) depending on membrane potential. The fluorescence of 10,000 cells was recorded upon excitation at fluorescent emission shift of JC-1 from Red (~590 nm) to green (~529 nm), and evaluated by cytofluorimetry (FACScalibur, Becton Dickinson, Mountain View, CA, USA) with 488 excitations lasers as previously described [23].

2.6. Cell Apoptosis

Cell apoptosis was evaluated in cells cultured at submerged conditions stimulated for 72 h with $CdCl_2$ (0, 1, 10, 100 nM, 1 and 10 µM) for dose response or with $CdCl_2$ (100 nM) and $CdCl_2$ (100 nM)/BDEs (47a) (100 nM) mixtures or $CdCl_2$ (100 nM)/BDEs (209) (100 nM) mixtures. Briefly, cells were stained with a solution containing a mixture of Annexin V-FITC in binding buffer 1×. After incubation (15 min in total darkness, RT), Propidium Iodide was added just before analysis. The number of viable apoptotic cells was determined by cytofluorimetry (FACScalibur, Becton Dickinson, Mountain View, CA, USA) [23].

2.7. DNA Damage Analysis

Comet assay was performed as previously described [23,29] in A549 cells exposed for 72 h to $CdCl_2$ (100 nM) and $CdCl_2$ (100 nM)/BDEs (47 and −209) (100 nM) mixtures. After incubation, the cell suspension was then layered on one-third frosted slides pre-coated, OxiSelectTM Comet Assay Kit Cat. N. STA- 35 (Cell Biolabs, Inc., San Diego, CA, USA). The cells were lysed and subjected to electrophoresis at 0.7 V/cm for 30 min. The Comet images were acquired at 10× magnification by using a fluorescence microscope (Zeiss) and subjected to image analysis using Image J. The DNA damage was quantified by measuring the displacement between the genetic material of the nucleus ('Comet head') and the resulting 'tail". Tail moment length (µm), Tail DNA intensity and Cell DNA intensity were taken by the operator using image analysis, to evaluate Tail DNA% (100 × Tail DNA Intensity/Cell DNA Intensity) and then were used to calculate Olive Tail Moment (OTM) by the formula Tail DNA % × Tail Moment Length.

2.8. Measurement of TJ Integrity by TEER

TJ integrity was evaluated in ALI culture, measuring TEER values before (TEER pre) and after 72 h of stimulation (TEER post), as previously described with minor modifications [10,30]. A total of 500 µL of pre-warmed PBS was added in the apical compartment (10 min at 5% CO_2, 37 °C), and TEER values were measured. After the measurement of TEER pre, the apical solution was removed, and ALI cultures were stimulated. TEER post-stimulation was measured, the apical wash was discharged and the membranes of transwell inserts (0.4 mm pore size) were cut out and processed for protein extraction and RNA isolation, as described below.

2.9. Total Protein Extraction

Cells were washed with cold PBS and lysed in a buffer containing 10 mmol/L Tris-HCl (pH 7.4), 50 mmol/L NaCl, 5 mmol/L ethylenediaminetetraacetic acid (EDTA), 1% Nonidet P-40; phosphatase inhibitors consisted of 20 mmol/L b-glycerophosphate, 0.3 mmol/L Na3VO4 and 1 mmol/L Benzamidine (ICN Biochemicals, Inc., Aurora, OH, USA); protease inhibitors consisted of complete protease inhibitor cocktail (Roche), as previously described [30]. The protein content of the supernatants was analyzed using a bicinchoninic acid (BCA) assay (Pierce, Rockford, Ill); 25–30 μg of lysate was then denatured under reducing conditions by boiling for 10 min in 50 mM Tris-HCl (pH 6.8), 1% sodium dodecyl sulfate (SDS) and 0.01% bromophenol blue. Total protein extracts were analyzed by Western blot.

2.10. Western Blot Analyses

Proteins were separated by SDS and polyacrylamide gel electrophoresis (PAGE) and transferred by electrophoresis onto Immobilon-P membranes (Millipore, Bedford, MA, USA) as previously described [30]. Briefly, after transfer, the membranes were blocked overnight at room temperature in PBS containing 3% BSA and 0.5% Tween 20 before being incubated for 1 h at room temperature with the primary Abs. After washing, the blot was incubated for 45 min with the appropriate horseradish peroxidase-conjugated secondary Ab; bound Ab was detected using the ECL chemiluminescence detection system (Amersham-Pharmacia, Biotech, MI, Italy), according to the manufacturer's instructions. Membranes were stripped and reprobed with housekeeping proteins anti-β-actin Ab to normalize differences in protein loading.

2.11. Western Blot Antibodies

The following Abs were used: anti-nicotinamide adenine dinucleotide phosphate (NAPDH) oxidase 4 rabbit monoclonal antibody (NOX-4) (ab133303, Abcam, Cambridge, UK) (1:500), anti-NRF2 (D1Z9C) rabbit monoclonal antibody (12721, Cell Signaling Technology, Danvers, MA, USA) (1:200), an anti-TFAM (D5C8) rabbit monoclonal (8076, Cell Signaling Technology) (1:200) and a rabbit polyclonal anti-phospho-human γH2AX (Ser 139) Ab (07-164, Merck Millipore, Milan, Italy) (1:100 dilution).

2.12. Gel Images Evaluation

Autoradiography films were scanned by means of densitometry and analyzed with Image/Gel Plotting analysis software (National Institutes of Health, Bethesda, MD, USA) to determine band intensities. Data are expressed as arbitrary densitometric units (A.D.U.) corrected against the density of β-actin bands.

2.13. Immunofluorescence for γH2AX Foci Formation

γH2AX foci were used to identify the presence of $CdCl_2$ and BDEs- induced DNA double-strand breaks as previously described [29–32] with minor modifications [33]. The cells grown on -2-well chamber slides were exposed to $CdCl_2$ (100 nM) and $CdCl_2$ (100 nM)/BDEs (47 and −209) (100 nM) mixtures for 72 h. The cells were then fixed in 4% paraformaldehyde for 10 min, permeabilized with 0.2% Triton X-100 for 5 min and blocked with 1% BSA for 1 h. Cells were then incubated with anti-phospho-H2AX (ser 139) antibody, overnight at 4 °C and incubated with anti-rabbit FITC (F7512, Sigma-Aldrich, St. Louis, MO, USA) for 1 h. Hoechst 33,342 (Sigma-Aldrich, Inc., Milan, Italy) 1:1000 in PBS for 10 min at room temperature was used to stain nuclei, followed by a wash in PBS. The slides were mounted using Vectashield mounting medium (Vector Laboratories, Burlingame, CA, USA), and the fluorescence was visualized using a laser-scanning microscope ZEISS at a final magnification of 63, Scale bar 20 μm [23].

2.14. RNA Isolation and Quantitative RT-PCR (ZO-1, Claudin-1 and E-Cadherin-1)

Total RNA was extracted from A549 cells in ALI culture using TRIzol Reagent (Invitrogen) following the manufacturer's instructions. Then, it was reverse-transcribed into

complementary DNA (cDNA), using M-MLVRT and oligo (dT)12e18 primer (Invitrogen). Quantitative real-time PCR of the ZO-1, Claudin-1 and E-Cadherin transcripts was carried out in a StepOne Plus Real-time PCR System (Applied Biosystems, Foster City, CA, USA) using specific FAM labeled probe and primers (prevalidated TaqMan Gene expression assay for ZO-1 (Hs01551861_m1, Claudin-1 (Hs 00221623_m1) and E-Cadherin (Hs 01023895_m1) and with a dye label VIC for GAPDH (Hs 02786624_g1) were purchased from Thermo Fisher Scientific (Pleasanton, CA, USA). ZO-1, Claudin-1 and E-Cadherin gene expression were normalized to GAPDH endogenous control gene. The relative quantitation of gene expression was performed with the comparative CT method (2DDCt) and plotted as fold-change compared with untreated cells as the reference sample [10].

2.15. Morphological Evaluation

Morphological changes of A549 stimulated with cadmium and BDE congeners (100 nM concentration) were recorded by light microscopy (Leica microscope, Wentzler, Germany) at 20× of magnification.

2.16. Statistical Analysis

Kolmogorov–Smirnov normality test was performed to assess normal data distribution. Analysis of variance (ANOVA) corrected with Fisher's test and paired *t*-test analysis were used for comparisons. Data are expressed as mean ± standard deviation (S.D.) All statistical analyses were performed using StatView® 5 software (SAS institute Inc., Cary, North Carolina, USA). A p-value < 0.05 was considered to be statistically significant.

3. Results

3.1. Cytotoxic Effects of $CdCl_2$ and $CdCl_2$/BDE Mixtures in Submerged Culture of A549 Cells

Submerged culture of A549 cells exposed to different concentrations of $CdCl_2$ (1, 10, 100 nM,1 µM and 10 µM) for 72 h did not significantly induce alteration of cell metabolism or viability when compared with untreated cells; however, the A549 cells stimulated with a higher concentration of $CdCl_2$ (10 µM) showed a significant reduction in cell viability by MTS assay (Figure 1A).

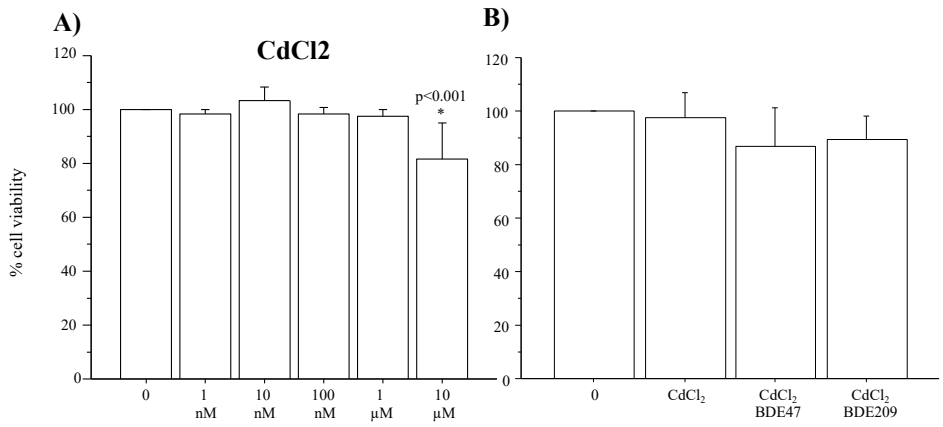

Figure 1. Cytotoxic effects of $CdCl_2$ and BDEs in submerged culture of A549 cells. A549 were stimulated for 72 h with different concentrations of (**A**) $CdCl_2$ (1, 10, 100 nM, 1 and 10 µM) and with (**B**) $CdCl_2$ (100 nM) and $CdCl_2$/BDE-47 or $CdCl_2$/BDE-209 (100 nM) to evaluate cell viability by MTS assay. Bars represent mean ± S.D. of separate experiments; (**A**) n = 6 and (**B**) n= 4. Statistical analysis was performed by ANOVA test with Fisher's correction for multiple comparisons. * Significance was set at $p < 0.05$.

Furthermore, $CdCl_2$ (100 nM)/BDE-47 (100 nM) mixture or $CdCl_2$ (100 nM)/BDE-209 (100 nM) mixture did not significantly decrease cell viability in A549 cells compared to untreated cells. No additional effect was observed in A549 cells stimulated with $CdCl_2$

(100 nM)/BDE-47 (100 nM) or $CdCl_2$ (100 nM)/BDE-209 (100 nM) mixtures, when compared to the cells treated with single $CdCl_2$ (Figure 1B). The effect of BDE-47 or BDE-209 (100 nM) alone was previously described [23] and here, the data are not shown.

3.2. Effect of $CdCl_2$ Treatment on ROS Production and Mitochondrial Injury in Submerged Culture of A549 Cells

To establish whether $CdCl_2$ stimulates intracellular oxidative stress, we examined ROS levels based on DCFH-DA fluorescence using flow cytometry. The incubation of the cells with $CdCl_2$ 100 nM and 1 µM for 4 h significantly increased intracellular ROS formation in A549 cells compared to untreated cells (Figure 2A,B).

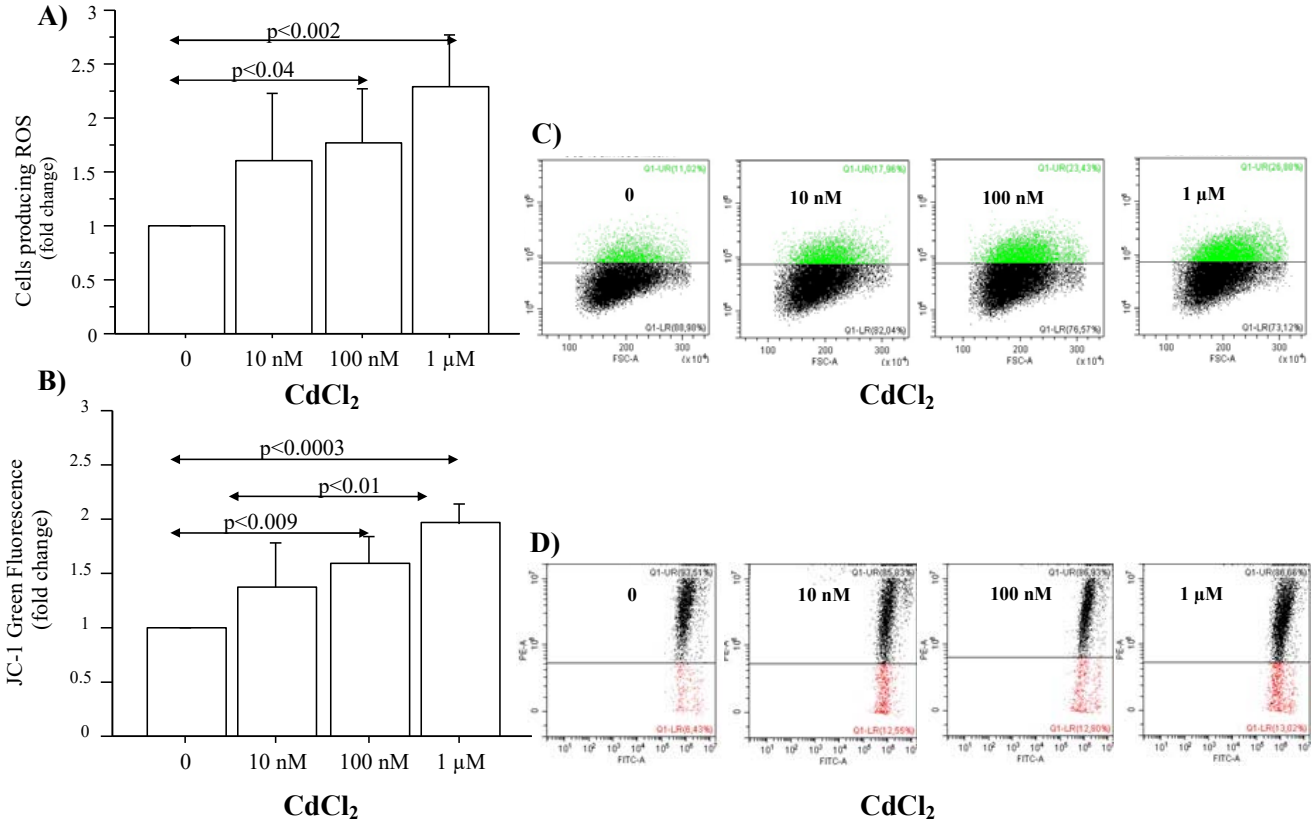

Figure 2. Effect of $CdCl_2$ on ROS and JC-1 in submerged culture of A549 cells. A549 were stimulated for 4 h with $CdCl_2$ (10, 100 nM and 1 µM) and analyzed for (**A**) ROS production and (**B**) JC-1 (Green fluorescence) by flow cytometry. Representative flow cytometric analysis is shown for (**C**) ROS and (**D**) JC-1. Bars represent mean ± S.D of Gated (%) of 4 different experiments expressed as fold change (obtained choosing untreated cells as reference sample). Statistical analysis was performed by ANOVA test with Fisher's correction for multiple comparisons. Significance is accepted at $p < 0.05$.

Cell stress showed a decrease in the potential membrane mitochondrial and an increase of JC-1 (monomers) green fluorescence (MMP decreases). Accordingly, we found that $CdCl_2$ (100 nM and 1 µM) significantly increased JC-1 in submerged A549 cells compared to untreated cells (Figure 2C,D). The effect of BDE-47 or BDE-209 (100 nM) alone was previously described [23] and here, the data are not shown.

3.3. Effects of $CdCl_2$ and $CdCl_2$/BDE Mixtures on ROS Production, Mitochondrial Injury and Apoptosis in A549 Cells

$CdCl_2$ (100 nM) significantly increased intracellular ROS formation and JC-1 green fluorescence in submerged culture of A549 cells compared to untreated cells. The stimulation of the cells with $CdCl_2$/BDE-47 or $CdCl_2$/BDE-209 mixtures did not affect additional

differences in ROS and JC-1 formation when compared to the cells stimulated with $CdCl_2$ (Figure 3).

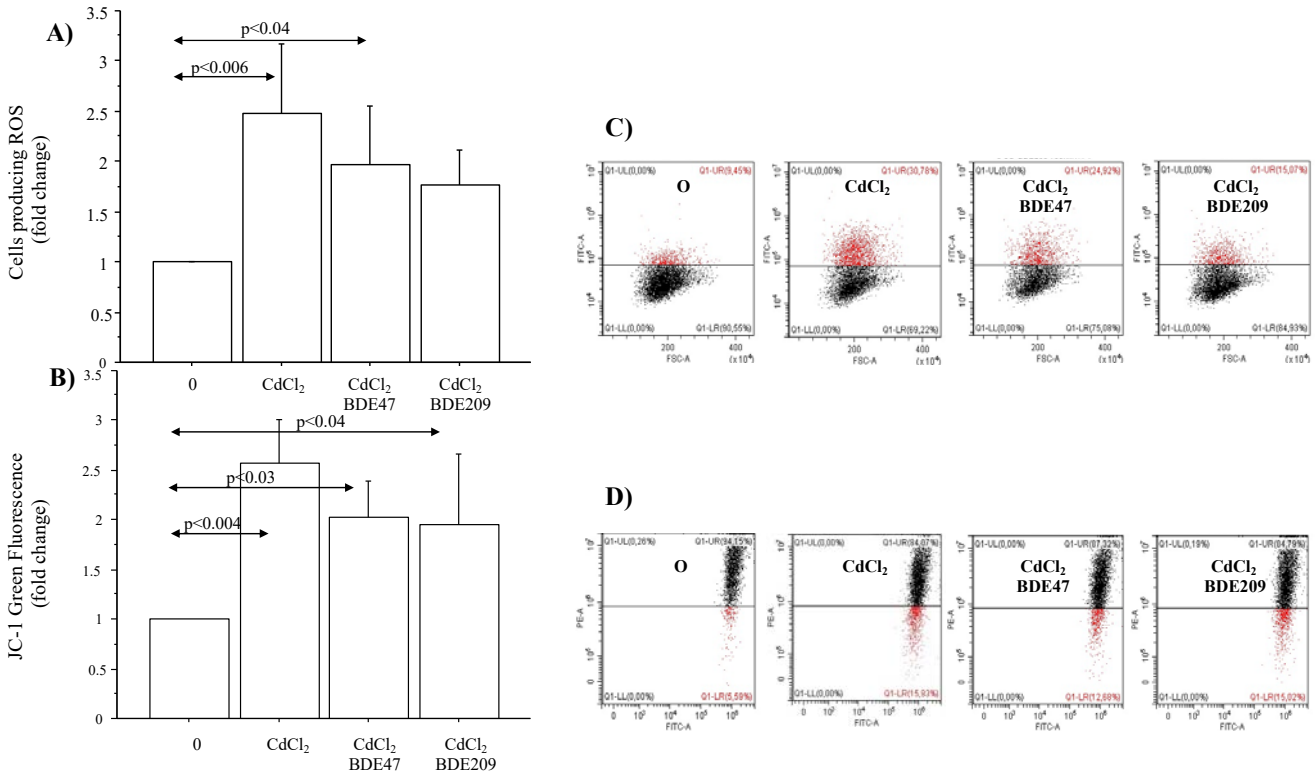

Figure 3. Effects of $CdCl_2$ and BDE mixtures on ROS and JC-1 in submerged culture of A549 cells. A549 were stimulated for 4 h with single $CdCl_2$ (100 nM) or with $CdCl_2$/BDE-47 and $CdCl_2$/BDE-209 and analyzed for (**A**) ROS production and (**B**) JC-1 (Green fluorescence) by flow cytometry. Representative flow cytometric analyses are shown for (**C**) ROS and (**D**) JC-1. Bars represent mean ± S.D. of Gated (%) of 4 different experiments expressed as fold change (obtained choosing untreated cells as reference sample). Statistical analysis was performed by ANOVA test with Fisher's correction for multiple comparisons. Significance is accepted at $p < 0.05$.

The stimulation of the cells with different concentrations of $CdCl_2$ (0 to 10 µM) show that only $CdCl_2$ 10 µM significantly increased cell apoptosis (Anx^+PI^- + Anx^+PI^+) (early + later apoptosis) in submerged culture of A549 cells compared to untreated cells or to the cells stimulated with lower concentrations of $CdCl_2$ (Figure 4A,B).

The stimulation of A549 cells with $CdCl_2$ (100 nM) for 72 h did not increase the percentage of apoptotic cells; however, $CdCl_2$ (100 nM)/BDE-47 (100 nM) or $CdCl_2$ (100 nM)/BDE-209 (100 nM) significantly increase the percentage of apoptotic cells compared to the cells treated with $CdCl_2$ or to untreated cells (Figure 4C,D). The effect of BDE-47 or BDE-209 (100 nM) alone was previously described [23] and accordingly, here, the data are not shown.

3.4. Effect of $CdCl_2$ and $CdCl_2$/BDE Mixtures on DNA Damage/Repair Mechanisms in A549 Cells

A single-cell gel electrophoresis assay was conducted to determine broken DNA, liberated from the Comet heads, after the treatment of the cells with $CdCl_2$ (100 nM) or with $CdCl_2$ (100 nM)/BDE-47 (100 nM) and $CdCl_2$ (100 nM)/BDE-209 (100 nM) mixtures for 72 h. $CdCl_2$ or $CdCl_2$ (100 nM)/BDE-47 (100 nM) and $CdCl_2$ (100 nM)/BDE-209 (100 nM) mixtures significantly induced Olive Tail Moment in A549 cells (Figure 5A,B) than in untreated cells.

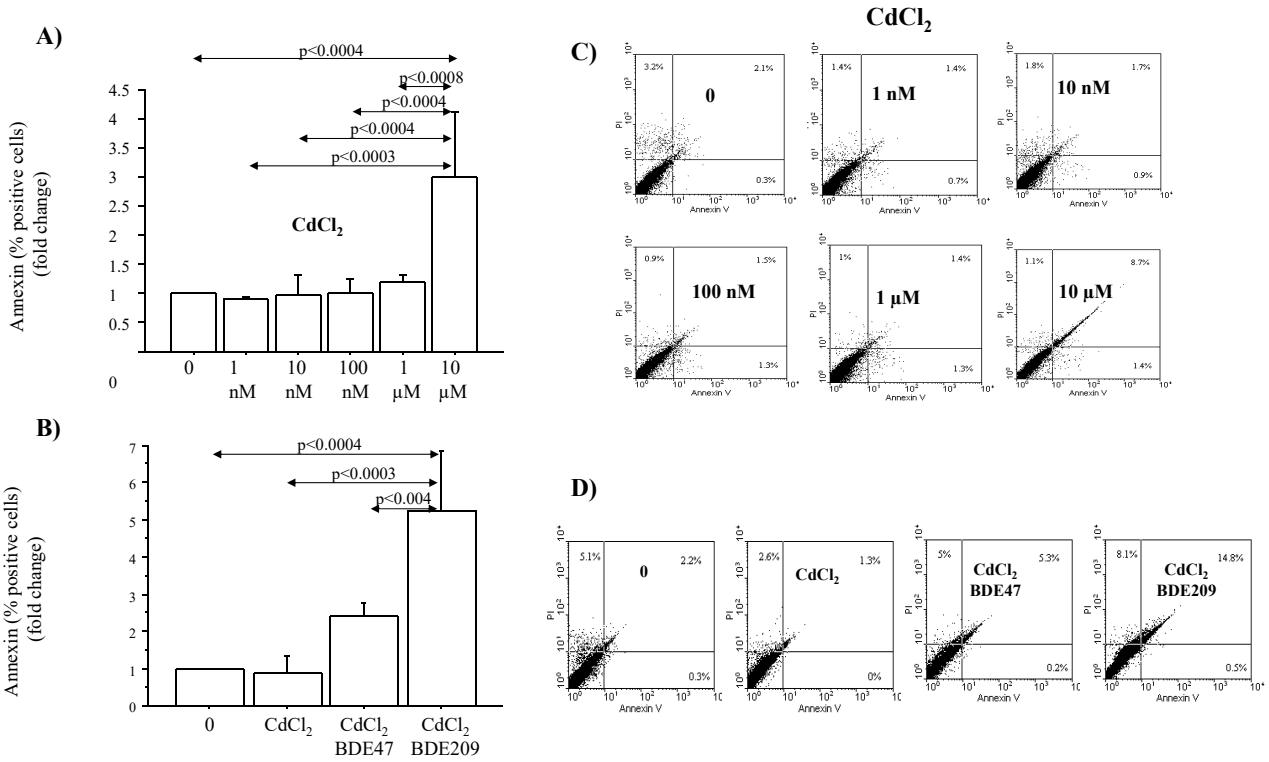

Figure 4. Effect of $CdCl_2$ and BDEs on cell apoptosis in submerged culture of A549 cells. A549 were stimulated for 72 h with (**A**) $CdCl_2$ (1, 10, 100 nM and 1, 10 µM) for dose response, and with (**B**) single $CdCl_2$ (100 nM) and $CdCl_2$/BDE-47 and $CdCl_2$/209 and analyzed for apoptotic cells (Anx^+PI^- + Anx^+PI^+). (**C**,**D**) Representative flow cytometric analysis is shown. Bars represent mean ± S.D of Gated (%) of 3 different experiments of apoptotic cells (Anx^+PI^- + Anx^+PI^+) expressed as fold change (obtained choosing untreated cells as reference sample). Statistical analysis was performed by ANOVA test with Fisher's correction for multiple comparisons. Significance is accepted at $p < 0.05$.

No additional increase was observed in the cells stimulated with mixtures and compared to the cells stimulated with single $CdCl_2$. The distribution of DNA damage variation is shown in Table 1.

Table 1. Table of the frequency of the tail length (distribution of varying level of damage DNA in term of tail length (mm)) showing DNA damage.

A549 Cells	1	2	3	4	5	Frequency Classes Lenght (µm)
						1 = 0 - 20
0	117	32	1	0	0	2 = 21 - 40
$CdCl_2$	95	27	21	7	0	3 = 41 - 60
$CdCl_2$ + BDE 47	81	29	21	19	0	4 = 61 - 80
$CdCl_2$ + BDE 209	69	27	24	28	2	5 = 81 - 100

The effect of BDE-47 or BDE-209 (100 nM) alone was previously described [23] and accordingly, here, the data are not shown.

We first investigated the impact of persistent oxidative stress on protein by Western blot analysis of whole-cell extracts from A549 submerged cells stimulated for 72 h. $CdCl_2$ (100 nM) or with $CdCl_2$ (100 nM)/BDE-47 (100 nM) and $CdCl_2$ (100 nM)/BDE-209 (100 nM) mixtures induced a significant increase of γH2AX phosphorylation in the stimulated cells rather than in untreated cells (Figure 6A).

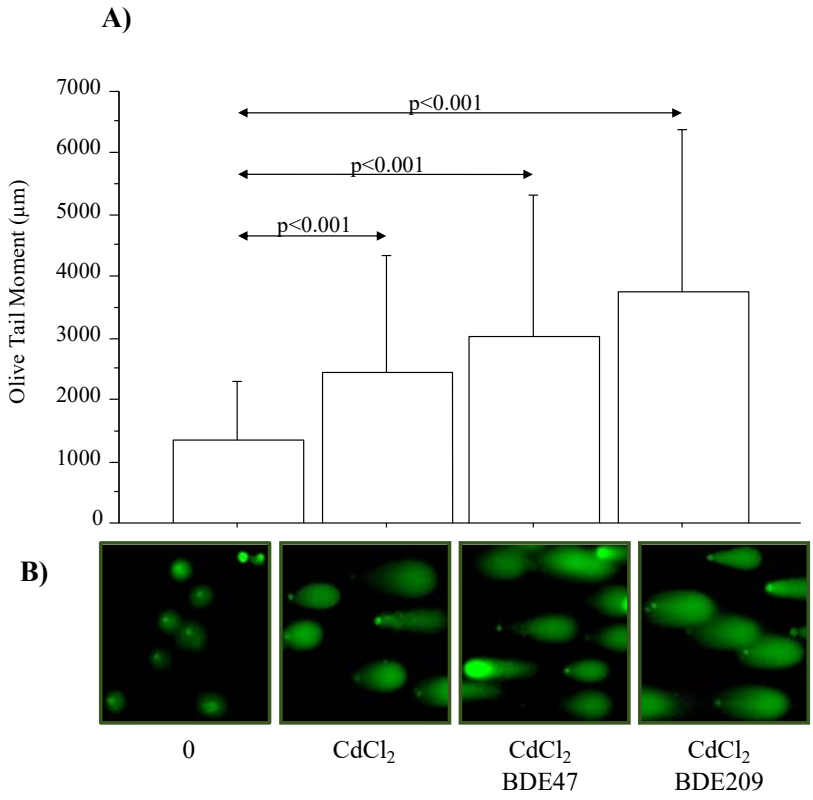

Figure 5. Genotoxic effect of $CdCl_2$ and BDEs on DNA damage/repair mechanisms in submerged culture A549 cells. A549 were stimulated with single $CdCl_2$ (100 nM) and with $CdCl_2$ (100 nM)/BDE-47 and $CdCl_2$ (100 nM)/BDE-209 (100 nM) concentration for 72 h to evaluate (**A**) Genomic DNA damage detected by the alkaline Comet assay. (**B**) Representative Comet images showing DNA damage by $CdCl_2$, and $CdCl_2$/BDEs congeners are shown. Images were acquired by using laser scanning microscope ZEISS at a final magnification of 10×. Statistical analysis was performed by ANOVA test with Fisher's correction for multiple comparisons. Significance is accepted at $p < 0.05$.

Additionally, we described the effect of $CdCl_2$(100 nM)/BDE-47(100 nM) and $CdCl_2$ (100 nM)/BDE-209 (100 nM) mixtures on the presence of nuclear γH2AX by immunofluorescence to detect nuclear foci. $CdCl_2$ and $CdCl_2$ (100 nM)/BDE-47 (100 nM) or $CdCl_2$ (100 nM)/BDE-209 (100 nM) mixtures increased the presence of γH2AX DSB reparation foci in the stimulated cells rather than in untreated cells (Figure 6B). The effect of BDE-47 or BDE-209 (100 nM) alone on phosphorylated γH2AX was previously described [23] and accordingly, here, the data are not shown.

3.5. Cytotoxic Effects and NOX-4, Nrf2 and TFAM Protein Expression in ALI Culture of A549 Cells Exposed to $CdCl_2$ and $CdCl_2$/BDE Mixtures

A549 cells cultured in ALI system and stimulated with different concentrations of $CdCl_2$ (from 1 nM to 10 µM) for 72 h showed a significant reduction in cell viability only with $CdCl_2$ 10 µM using MTS assay (Figure 7A).

Furthermore, $CdCl_2$ and $CdCl_2$ (100 nM)/BDE-47 (100 nM) or $CdCl_2$ (100 nM)/BDE-209 mixtures did not decrease cell viability in A549 cells compared with untreated cells (Figure 7B).

We explored NOX-4 protein expression in ALI culture of A549 cells treated with $CdCl_2$ (100 nM) and $CdCl_2$/BDE-47 or $CdCl_2$/BDE-209 mixtures for 72 h. As shown in Figure 8A, the treatment of the cells with $CdCl_2$ and $CdCl_2$/BDE-47 or $CdCl_2$/BDE-209 mixtures significantly enhanced the expression of NOX-4 in comparison with untreated cells (Figure 8A).

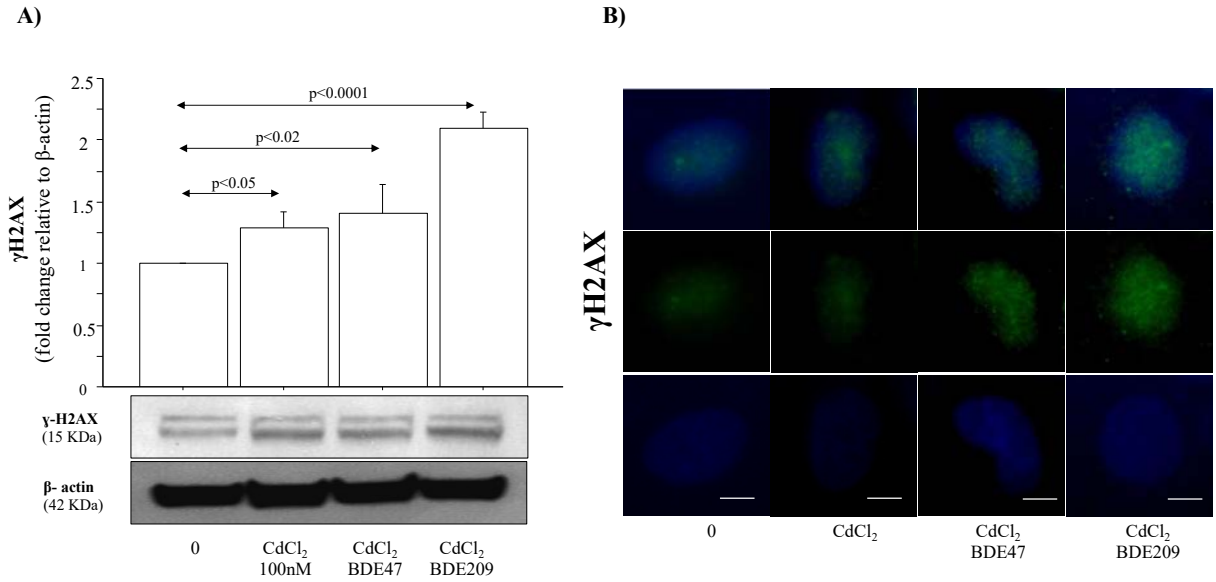

Figure 6. Effect of $CdCl_2$ and BDEs on repair mechanisms in submerged culture of A549 cells. A549 were stimulated with single $CdCl_2$ (100 nM) and with $CdCl_2$ (100 nM)/BDE-47 and $CdCl_2$ (100 nM)/BDE-209 (100 nM) concentration for 72 h to evaluate γH2AX phosphorylation (Ser139) (**A**) by Western blot analysis; (**B**) the presence of γH2AX foci by immunofluorescence. Bars represent mean ± S.D. of arbitrary densitometric units (ADU) corrected against the density of β-actin (n = 3). Data were plotted as fold change obtained, choosing baseline cells as reference samples. Representative gel images of γH2AX (ser139) and β-actin are shown. The stimulated cells were fixed and stained with anti γH2AX antibody (Green fluorescence) and subjected to immunofluorescent microscopy. Cell nuclei were stained with Hoechst 33,342 (Blue fluorescence). Representative images analysis of γH2AX are shown at magnification 63×.

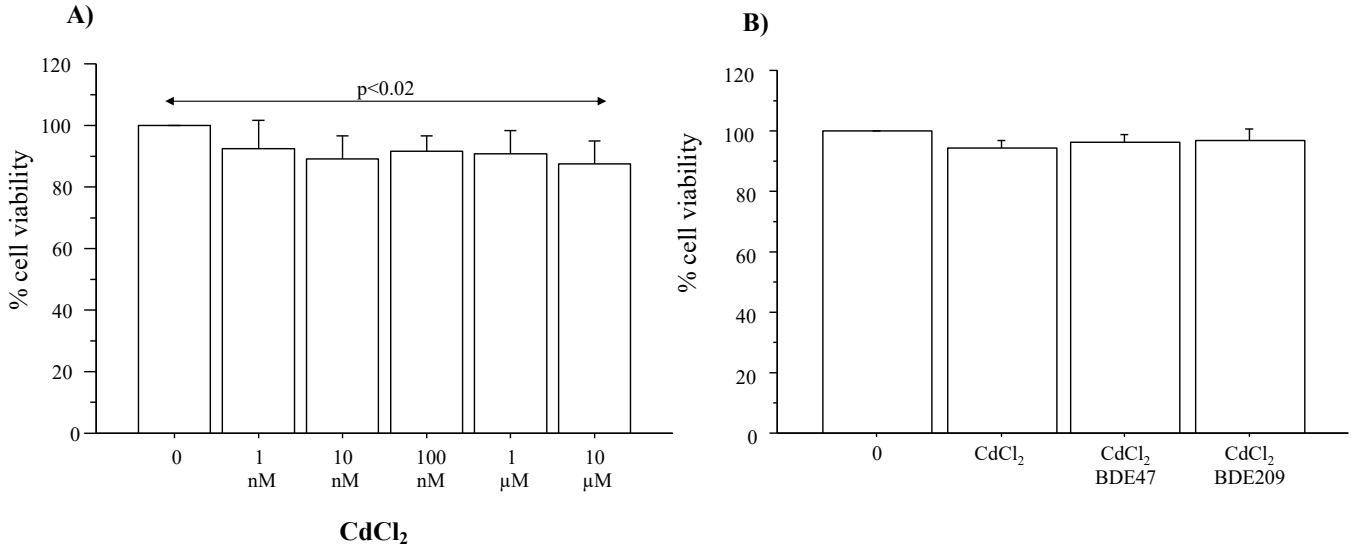

Figure 7. Cytotoxic effects of $CdCl_2$ and BDEs in ALI culture of A549 cells. A549 cells were stimulated for 72 h (**A**) with different concentrations of single $CdCl_2$ (1, 10, 100 nM, 1 and 10 μM), and with (**B**) $CdCl_2$ (100 nM) or $CdCl_2$ (100 nM)/BDE-47 and $CdCl_2$ (100 nM)/BDE-209 (100 nM) concentration to evaluate cell viability by MTS Assay. Bars represent mean ± S.D. of n = 4 separate experiments. Statistical analysis was performed by ANOVA test with Fisher's correction for multiple comparisons. Significance was set at $p < 0.05$.

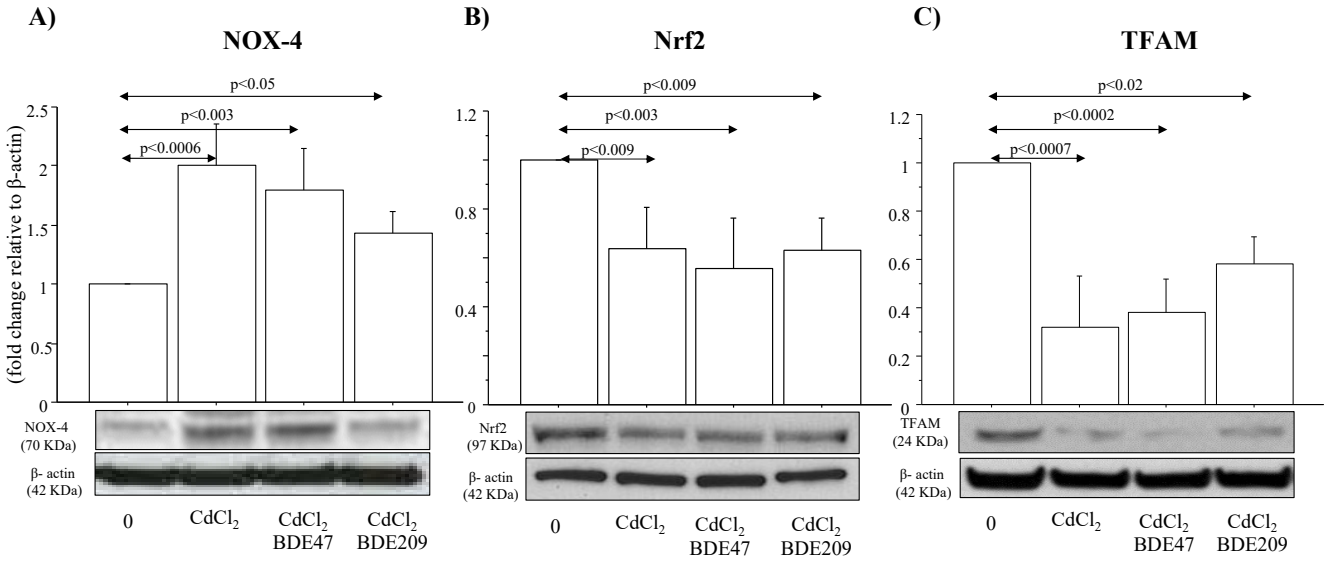

Figure 8. Effects of $CdCl_2$ and BDEs stimulation on NOX-4, Nrf-2 and TFAM protein expression on ALI A549 cells. The cells were stimulated for 72 h with single $CdCl_2$ (100 nM) or with $CdCl_2$ (100 nM)/BDE-47 and $CdCl_2$ (100 nM)/BDE-209 (100 nM) to evaluate (**A**) NOX-4, (**B**) Nrf2 and (**C**) TFAM protein expression in whole lysates by Western blot. Bars represent mean ± S.D. of arbitrary densitometric units (ADU) corrected against the density of β-actin (n = 3). Data were plotted as fold change obtained, choosing untreated cells as reference sample. Representative gel images of NOX-4, Nrf2, TFAM, and β-actin are shown. Statistical analysis was performed by ANOVA test with Fisher's correction for multiple comparisons. Significance is accepted at $p < 0.05$.

Furthermore, the treatment of the cells with $CdCl_2$ and $CdCl_2$/BDE-47 or $CdCl_2$/BDE-209 mixtures for 72 h significantly decreased Nrf2 and TFAM expression in comparison with untreated cells (Figure 8B,C). The effect of BDE-47 or BDE-209 (100 nM) alone on NOX-4 was previously described [9], and accordingly, here, the data are not shown.

3.6. TEER and ZO-1, Claudin-1 and E-Cadherin mRNA and Protein Expression in ALI Culture of A549 Cells Exposed to $CdCl_2$ and $CdCl_2$/BDE Mixtures

TEER post-stimulation was significantly lower in the ALI culture of A549 cells exposed to $CdCl_2$ (100 nM, 1 and 10 μM) for 72 h in comparison with TEER pre-stimulation (Figure 9A).

No differences were shown between TEER pre and post in baseline conditions. The levels of Delta TEER were not significantly different in ALI culture of A549 exposed to $CdCl_2$ and to $CdCl_2$/BDE-47 or $CdCl_2$/BDE-209 mixtures than in untreated cells (Figure 9B). The effect of BDE-47 or BDE-209 (100 nM) alone on TEER measurements was previously described [10], and accordingly, here, the data are not shown.

ZO-1, Claudin-1 and E-Cadherin proteins are proteins that well-characterized the role of tight junctions in the integrity of the epithelial layer. ZO-1, Claudin-1 and E-Cadherin mRNA expression was detected in ALI culture of A549 cells stimulated with $CdCl_2$ (100 nM) and $CdCl_2$ (100 nM)/BDE-47 (100 nM) or $CdCl_2$ (100 nM)/BDE-209 (100 nM) for 72 h by RT-qPCR (in total RNA). ZO-1, Claudin-1 and E-Cadherin significantly decreased in the cells stimulated with $CdCl_2$ and with $CdCl_2$/BDE-47 or with $CdCl_2$/BDE-209 mixtures compared to untreated cells. The effect of BDE-47 or BDE-209 (100 nM) alone was previously described on barrier integrity [9] and accordingly, here, the data are not shown.

The analyses of ZO-1, Claudin-1 and E-Cadherin proteins by immunofluorescence assay support the data on the levels of transcripts. Interestingly, immunofluorescence staining pointed out that exposure of A549 under ALI culture to $CdCl_2$ (100 nM) and $CdCl_2$ (100 nM)/BDE-47 (100 nM) and $CdCl_2$ (100 nM)/BDE-209 (100 nM) affected the expression of ZO-1, Claudin-1 and E-cadherin (Figure 10).

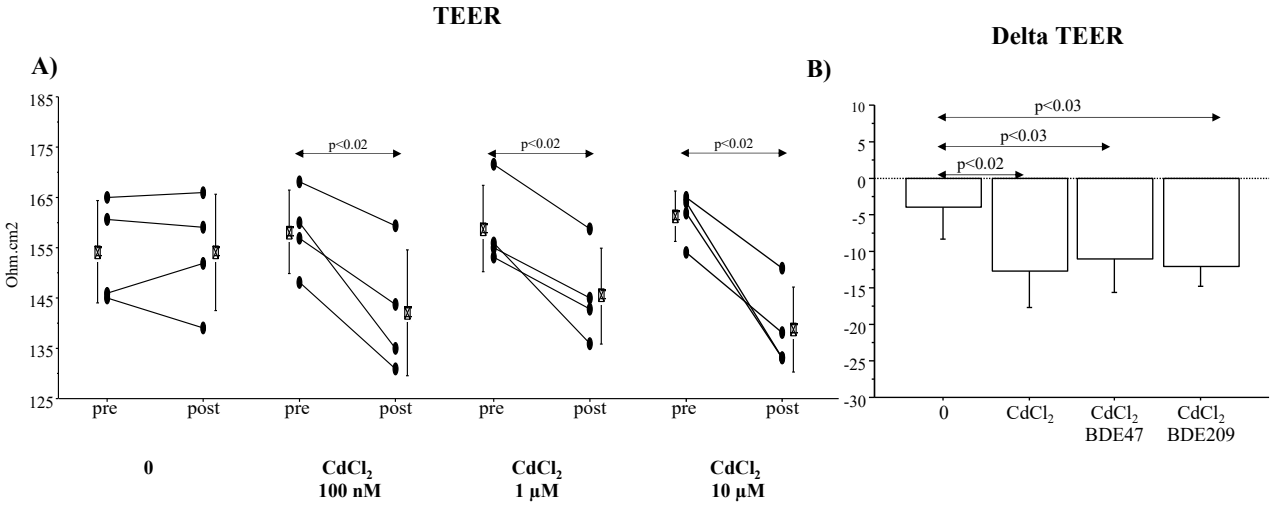

Figure 9. Evaluation of integrity barrier on ALI culture of A549 cells. A549 were grown in ALI culture for 5 days and stimulated for 72 h (**A**) with different concentrations of $CdCl_2$ (100 nM, 1 and 10 µM) to evaluate TEER pre and post-stimulation (n = 4); (**B**) with $CdCl_2$ (100 nM) and with $CdCl_2$ (100 nM)/BDE-47 and $CdCl_2$ (100 nM)/BDE-209 (100 nM) to evaluate Delta TEER (post minus pre-stimulation) (n = 4). The final dilution of $CdCl_2$ and BDEs (−47 and −209) contains 0.05% of DMSO. The same % of DMSO was added to the baseline as a vehicle. Statistical analysis was performed by Student's *t*-test. Significance was at $p < 0.05$. Bars represent mean ± S.D. of Delta TEER. Statistical analysis was performed by ANOVA followed by Fisher's PLSD correction. Significance was at $p < 0.05$.

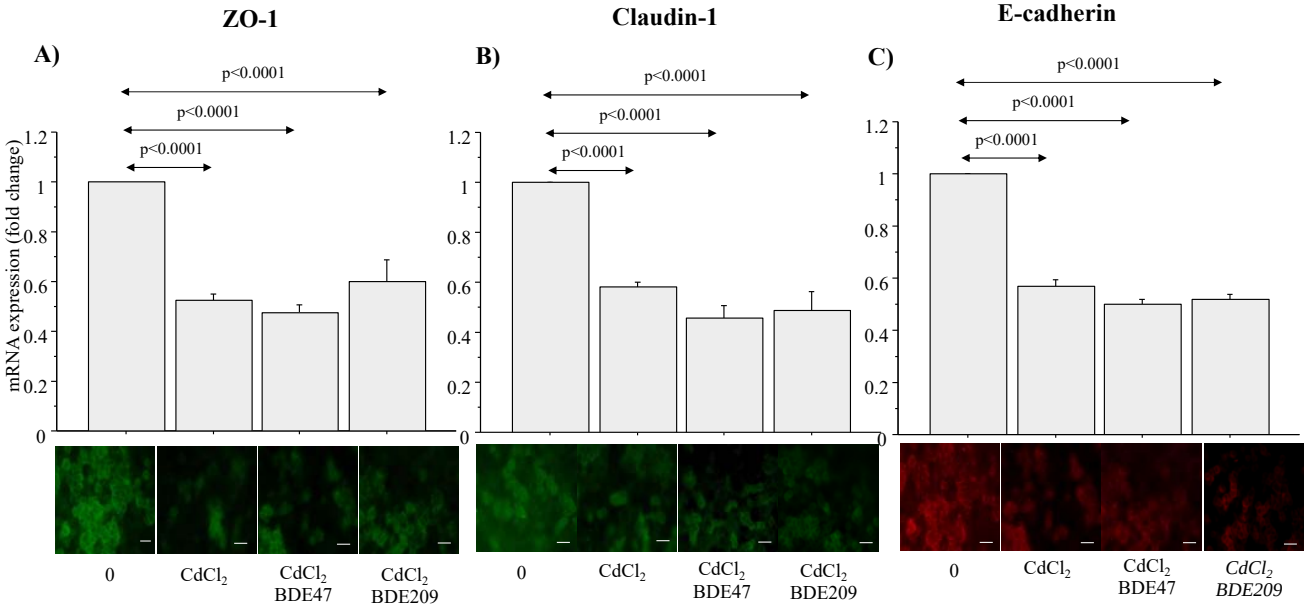

Figure 10. Effect of $CdCl_2$ and BDEs on AJ and TJ in ALI culture of A549 cells. A549 were grown in ALI culture for 5 days and treated for 72 h with $CdCl_2$ (100 nM) and with $CdCl_2$ (100 nM)/BDE-47 and $CdCl_2$ (100 nM)/BDE-209 (100 nM) to evaluate: (**A**) ZO-1 (n = 3), (**B**) Claudin-1 (n = 3) and (**C**) E-Cadherin (n = 3) mRNA expression by real-time PCR. The final dilution of $CdCl_2$ and BDEs (−47 and −209) contains 0.05% of DMSO. The same % of DMSO was added to the baseline as vehicle. Data are expressed as mean ± S.D. of separate experiments and data were plotted as fold change over baseline. Statistical analysis was performed by ANOVA followed by Fisher's PLSD correction. Significance was at $p < 0.05$.

4. Discussion

It is established that Cd or BDEs inhalation leads to several lung pathologies; however, the effect of the exposure to Cd together with BDE 47 or BDE 209 on the alterations of human health is partially studied and understood in airway diseases. Here, we reported for the first time the joint toxicity of Cd/BDE 47 or Cd/BDE 209 exposure on cell death, mitochondrial function, mechanisms of DNA damage/repair and barrier integrity in an in vitro model of airway epithelial cells obtained using submerged and ALI culture of A549 cell line. We observed that $CdCl_2$ might have adverse effects on human lung function damaging airway epithelial cell activities, without an additional or synergistic effect in the presence of BDE 47 or 209.

Cd is a typical toxic heavy metal and a persistent organic compound present, together with BDEs, in some areas of the world. The effects of contaminants are often manifested as imbalances in antioxidants [34], resulting in an increase in ROS production that could destroy the redox/balance and promote protein, DNA and lipid degradation [35]. Many studies have shown that environmental pollution due to Cd or BDEs plays a critical role in the pathophysiology of diseases, and the main cell mechanism responsible for their toxicity is oxidative stress. Detection of the environmental coexistence of Cd and BDEs increases public concern about their combined toxicity, which might be considered a higher health risk for humans and wildlife [36].

A549 cells were widely used in studies on human lung damage caused by toxic substances [36,37]. The use of A549 cell line culture is a widely used in vitro model to study the pathophysiological roles of BDEs in human lungs and to reproduce the effect of toxicants observed in cell cultures of primary bronchial epithelial cells [10,38]. First, we evaluated the potential effect of $CdCl_2$ and of $CdCl_2$/BDE mixtures on cytotoxic and genotoxic mechanisms using an in vitro model of A549 cells cultured in submerged conditions readily accessible, straightforward and practical. Then, we studied the effect of oxidative stress generated by $CdCl_2$ and by$CdCl_2$/BDEs mixtures on epithelial barrier integrity using the ALI culture system of A549, a 3D in vitro model of epithelium commonly useful to assess the effect of toxicant on the mechanism of cell-cell interactions [39].

Exposure to air pollutants injured the lung and epithelial cells are the first line of defense against exogenous molecules, playing a central role in pathophysiological mechanisms [2]. Single toxicological effects of Cd and BDE (47 or 209) have been recently studied in airway epithelium [2,10,23], but little is known about the effect of Cd and BDE (47 or 209) mixtures either in vivo or in vitro studies. Here, we showed that lower concentrations of single $CdCl_2$ (1 nM to 1μM), as well as the single CdCl2 (100 nM) in combination with BDE 47 or 209 (100 nM), did not cause a reduction in cell viability in submerged culture of A549 cells.

As previously described for BDE 47 and BDE 209 in human bronchial epithelial cell line [23], we showed here that $CdCl_2$ affect, in a dose-dependent manner, ROS production and mitochondrial membrane potential (JC-1 monomer) dysfunction in submerged culture of A549 cells. At the same time, in this study, we observed that single $CdCl_2$ in combination with BDE 47 or BDE 209 (100 nM) did not show an additional or synergistic increase in ROS production and dysfunction of mitochondrial membrane potential (JC-1). These findings show that there is no combined action of $CdCl_2$ and BDEs in the mechanism of oxidative stress of airway epithelium, supporting the concept that $CdCl_2$ or BDEs have high and equal levels of toxicity on human health of the lung.

$CdCl_2$-induced hepatotoxicity [40,41] and cytotoxicity of renal tubular epithelial cells, in duck [42] by ROS mediated dependent apoptosis pathway. The flame retardants (BFRs) such as BDEs play a primary role in the regulatory process of A549 cell line apoptosis through the mitochondrial pathway [43]. Many studies show that the mechanisms of cell transformation autophagy-associated are impaired by Cd [44,45] and trigger a wide range of responses related to immunity and oxidation (e.g., ROS, DNA damage, lipid peroxidation, cytokine overproduction, inflammation and proteostasis), damaging the epithelium lining the airways and alveoli [46,47]. Oxidative stress following BDE exposure

has also been related to autophagy induction [48] to defend the cells against further ROS and pro-apoptotic proteins production [49–51]. We showed here that different CdCl2 concentrations did not affect apoptosis in A549 cells; however, the combined stimulation of the cells with $CdCl_2$ (100 nM) and BDE-47 (100 nM) or BDE-209 (100 nM) had an additional effect on the A549 cell line apoptosis. Our findings suggest that oxidative stress dysfunction due to $CdCl_2$ might be associated with autophagy signaling suppressing apoptosis and BDEs alone (as previously described in Montalbano et al., 2020) or, in combination with $CdCl_2$, reverted this cell activity. These data open new perspectives toward further studies to clarify the mechanism of apoptosis in airway epithelial cells exposed to environmental chemicals as Cd and BDE-47 or BDE-209 mixtures.

Genotoxic and cytotoxic effects of toxicants can generate lung cancer. Detection of phosphorylated γH2AX and Comet assay is frequently used to evaluate the genotoxic effect of the substances on DNA damage/repair mechanisms. $CdCl_2$, through enhancement of ROS formation, induces damage to DNA macromolecules or cell cycle phase [52,53]. To resist DNA alteration, the cell initiates "DNA Damage Response", including a cohort of events such as arrest the cell cycle, apoptosis and γH2AX phosphorylation [54]. γH2AX (serine 139) phosphorylation occurs immediately after the formation of DNA double-strand breaks (DNA DSBs), signaling injury to the proteins responsible for DNA repair [55]. The phosphorylation of γH2AX is a fundamental step in the mechanisms of DNA damage [56]. The result is the production of detectable nuclear foci in euchromatin regions considered transcriptionally active in the mechanism of DNA repair [57–60]. The persistence of DNA lesions generates strand breaks corresponding to DNA migration by the Comet test. We show here that $CdCl_2$ induces γH2AX phosphorylation and immunofluorescent Comets in A549 cells. At the same time, the analysis of CdCl2 and BDEs (100 nM) mixtures effect show a slight increase in γH2AX phosphorylation and immunofluorescent Comet. Moreover, the immunofluorescence assay described the presence of nuclear foci in the cells showing γH2AX phosphorylation and Comets. Our findings might suggest that $CdCl_2$ generates the outbreaks of γH2AX phosphorylated and DSB signaling, promoting DNA lesions which in turn might be recognized as highly mutagenic lesions in the epithelium of the lung; however, we did not identify clear evidence to support that the combined exposure to CdCl2 and BDEs might have an additional effect on the mechanisms of DNA damage/repair of epithelial cells.

In cells, increased ROS production induces activation of autophagy to compensate for the excessive cell damage and death that result from oxidative stress [61]. NOX-4 serves as a gatekeeper in the regulation of autophagy activation through ROS production based on cell types and conditions [62,63]. Aberrant and excessive mechanisms of oxidative stress are involved in cellular/tissue injury and lead to pathological changes [49]. BDEs exert cytotoxic and genotoxic effects damaging the integrity of the airway epithelial barrier [10,23]. An increment in NOX-4 activity represses Nrf2 and TFAM proteins. Nrf2 is an oxidative stress-sensitive transcription factor and controls the expressions of antioxidant defense and detoxification genes [20]. Nrf2 plays a fundamental role in regulating mitochondrial function [64], and TFAM is important in the functional integrity of the mitochondrial respiratory chain and in the maintenance of balance between anti-oxidation and oxidation [65]. After the analysis of $CdCl_2$ or $CdCl_2$/BDE mixtures on cell viability in 3D ALI cultures of the A549 cell line, we studied oxidative stress and redox balance. We observed that $CdCl_2$ or $CdCl_2$/BDE mixtures affected the increase in NOX-4 and downregulated Nrf2 and TFAM expression, without any additional effect. These findings suggest that $CdCl_2$ might be involved in mitochondrial bioenergetics and biogenesis of NOX-4 ROS-dependent activities, repressing Nrf2 and TFAM endogenous antioxidant responses to cell stress of the stratified epithelium of the airways exposed to environmental pollution. Accordingly, with data on ROS or JC-1 activity observed in submerged culture of A549 cells, the expression of NOX-4, Nrf2 and TFAM did not show an additional or synergistic effect when the cells were stimulated with $CdCl_2$ and $CdCl_2$/BDEs mixtures. Once again, these findings show that there is no combined action of $CdCl_2$ and BDEs on the epithelial cells supporting the

concept that $CdCl_2$ or BDEs have high and equal levels of toxicity on human health of the lung; however, we suggest further study to describe mitochondrial oxygen consumption and ATP formation to better describe the action of $CdCl_2$ and $CdCl_2$/BDE mixtures on mitochondrial functions.

The effective function of the respiratory epithelium is a fundamental requirement to protect the airways from a wide range of exogenous inhaled substances. The mitochondrial function is important for the activities of the lung epithelium, such as barrier integrity, ciliary function and the regeneration of epithelial cells following injury [66]. The apical junctional complexes between neighboring cells are important to keep the epithelial barrier functioning in the lung. They are made up of tight apical junctions (TJs) proteins (Claudin family, Occludin or ZO-1 proteins) and adherent junctions (AJs) (E-cadherin) [67–69]. Interestingly to note that $CdCl_2$ or $CdCl_2$/BDE mixtures caused airway epithelial barrier dysfunction as demonstrated by TEER values reduction and simultaneously affecting ZO-1, Claudin-1 and E-cadherin mRNA and proteins expression. These findings suggested that $CdCl_2$ or $CdCl_2$/BDE mixtures caused airway epithelial barrier dysfunction by multiple TJ and AJ proteins downregulation; however, no additional or synergistic effect of $CdCl_2$ and $CdCl_2$/BDEs mixtures were found. These findings showed that $CdCl_2$ has a significant negative impact on the maintenance of the integrity barrier imparted by the airway epithelium. We believe that the central issue might be associated with autophagic dysfunction. Hence, a careful prospective analysis of autophagic activity can prevent or resolve the potentially toxic effects due to exposure to environmental contaminants. Furthermore, since cadherin adhesive function depends on the actin cytoskeleton, and this contribution to cell–cell adhesion is not fully understood [70], further study might be necessary to clarify and to elaborate the role of toxicants on actin cytoskeletal reorganization in epithelial cells of the airway; however, our observations might be considered an initial issue for a possible understanding of the real adverse effects associated with Cd and BDEs co-exposure of airway epithelial cells. In fact, although for some parameters there is no statistical significance, we observed a trend in γH2AX phosphorylation, NOX-4/TFAM protein expression and genomic DNA damage (Comet assay) changes in the epithelial cells stimulated with $CdCl_2$/BDE209 and compared to $CdCl_2$. These differences might suggest further investigation of the specific mechanism involved in γH2AX activity, NOX-4 and TFAM protein expression and DNA damage in the presence of environmental contaminants mixtures.

5. Conclusions

We concluded that $CdCl_2$ is a heavy metal involved in serious toxicities processes of the lung tissue and likewise BDEs as previously described [10,23]. Our investigation with respect to the toxicity of single $CdCl_2$ or $CdCl_2$/BDE mixtures showed an increase in ROS and JC-1 production, cell apoptosis and necrosis, DNA damage in terms of alkaline Comet assay and the presence of nuclear γH2AX foci in comparison to unexposed airway epithelial cells; however, the $CdCl_2$ and $CdCl_2$/BDE co-exposure might cause mitochondrial dysfunction and barrier integrity damage in the airway epithelium. Although our first idea was to demonstrate a combined effect of toxicant mixtures on the dysfunctional activities of epithelial cells, we showed here that $CdCl_2$/BDE47 or $CdCl_2$/BDE209 mixtures did not have a significative synergistic or additional effect compared to $CdCl_2$ alone on cytotoxic and genotoxic activities of airway epithelial cells; however, since we highlighted a changing trend induced by Cd and BDE-47 or BDE-209 mixtures, further investigation is needed in order to better understand these effects.

In this scenario, we concluded that the levels of toxicity generated individually by $CdCl_2$ or BDEs in airway epithelial cells are so high that the co-exposure to these substances does not generate further effects; however, due to the limits of the in vitro studies, to reinforce the message of our study, we suggest further in vivo epidemiological study to better clarify their combined negative action on human health of the lung.

Author Contributions: G.D.A. and M.P. conceived the study and designed the experiments. A.B., A.M.M., C.D.S., G.A., R.G. and S.R. performed the technical procedures. G.D.A. and M.P. provided data interpretation and wrote the paper. M.P. revised the final draft of the manuscript. All authors have read and agreed to the published version of the manuscript.

Funding: This study was funded by the International Centre of Advanced Study in Environment, ecosystem and human Health (CISAS), a multidisciplinary project on environment/health relationships funded by the Italian Ministry of Education, Universities and Research (MIUR) and approved by the Interministerial Committee for Economic Planning (CIPE)—body of the Italia Government—with Resolution no. 105/2015 of 23 December 2015.

Institutional Review Board Statement: Not applicable.

Conflicts of Interest: The authors of the paper declare that they have no competing interests for this study.

List of Abbreviations

$CdCl_2$	(Cadmium Chloride)
BDEs	(Brominated Diphenyl Ether flame-retardants)
ALI	(Air–Liquid Interface)
ROS	(Reactive Oxygen Species)
ZO-1	(Zonula Occludens-1)
NAPDH	Nicotinamide Adenine Dinucleotide Phosphate
NOX4	(NADPH oxidase 4)
TFAM	(Transcription Factor A, Mitochondrial)
Nrf2	(Nuclear factor erythroid 2–Related Factor 2)
TEER	(Trans epithelial/transendothelial electrical resistance)
DMSO	(Dimethyl sulfoxide)
DCFH-DA	(2, 7- dichloro-difluorescein diacetate)
EDTA	(ethylenediaminetetraacetic acid)
BCA	(bicinchoninic acid)
SDS	(sodium dodecyl sulfate)
PAGE	(polyacrylamide gel electrophoresis)
A.D.U.	(arbitrary densitometric units)
H2AX	(H2A histone family member X)

References

1. Agency for Toxic Substances and Disease Registry. *2019 Substance Priority List*; Agency for Toxic Substances and Disease Registry: Atlanta, GA, USA, 2019.
2. Rennolds, J.; Butler, S.; Maloney, K.; Boyaka, P.N.; Davis, I.C.; Knoell, D.L.; Parinandi, N.L.; Cormet-Boyaka, E. Cadmium regulates the expression of the CFTR chloride channel in human airway epithelial cells. *Toxicol. Sci. Off. J. Soc. Toxicol.* **2010**, *116*, 349–358. [CrossRef]
3. Gómara, B.; Herrero, L.; Ramos, J.J.; Mateo, J.R.; Fernández, M.A.; García, J.F.; González, M.J. Distribution of polybrominated diphenyl ethers in human umbilical cord serum, paternal serum, maternal serum, placentas, and breast milk from Madrid population, Spain. *Environ. Sci. Technol.* **2007**, *41*, 6961. [CrossRef] [PubMed]
4. Tang, Z.; Huang, Q.; Yang, Y.; Nie, Z.; Cheng, J.; Yang, J.; Wang, Y.; Chai, M. Polybrominated diphenyl ethers (PBDEs) and heavy metals in road dusts from a plastic waste recycling area in north China: Implications for human health. *Environ. Sci. Pollut. Res.* **2016**, *23*, 625–637. [CrossRef] [PubMed]
5. Zheng, H.; Hu, G.; Xu, Z.; Li, H.; Zhang, L.; Zheng, J.; Chen, L.; He, D. Characterization and distribution of heavy metals, polybrominated diphenyl ethers and perfluoroalkyl substances in surface sediment from the Dayan River, South China. *Bull. Environ. Contam. Toxicol.* **2015**, *94*, 503–510. [CrossRef] [PubMed]
6. Kim, J.-T.; Son, M.-H.; Lee, D.-H.; Seong, W.J.; Han, S.; Chang, Y.-S. Partitioning behavior of heavy metals and persistent organic pollutants among Feto–maternal bloods and tissues. *Environ. Sci. Technol.* **2015**, *49*, 7411–7422. [CrossRef] [PubMed]
7. Wang, L.; Zheng, M.; Gao, Y.; Cui, J. In vitro study on the joint hepatoxicity upon combined exposure of cadmium and BDE-209. *Environ. Toxicol. Pharmacol.* **2018**, *57*, 62–69. [CrossRef]
8. Leijs, M.M.; van Teunenbroek, T.; Olie, K.; Koppe, J.G.; ten Tusscher, G.W.; van Aalderen, W.M.; de Voogt, P. Assessment of current serum levels of PCDD/Fs, dl-PCBs and PBDEs in a Dutch cohort with known perinatal PCDD/F exposure. *Chemosphere* **2008**, *73*, 176–181. [CrossRef]
9. Ganesan, S.; Comstock, A.T.; Sajjan, U.S. Barrier function of airway tract epithelium. *Tissue Barriers* **2013**, *1*, e2. [CrossRef]

10. Albano, G.D.; Moscato, M.; Montalbano, A.M.; Anzalone, G.; Gagliardo, R.; Bonanno, A.; Giacomazza, D.; Barone, R.; Drago, G.; Cibella, F.; et al. Can PBDEs affect the pathophysiologic complex of epithelium in lung diseases? *Chemosphere* **2020**, *241*, 12. [CrossRef]
11. Hiemstra, P.S.; McCray, P.B., Jr.; Bals, R. The innate immune function of airway epithelial cells in inflammatory lung disease. *Eur. Respir. J.* **2015**, *45*, 1150–1162. [CrossRef]
12. De Rose, V.; Molloy, K.; Gohy, S.; Pilette, C.; Greene, C.M. Airway Epithelium Dysfunction in Cystic Fibrosis and COPD. *Mediat. Inflamm.* **2018**, *2018*, 130. [CrossRef] [PubMed]
13. Post, S.; Heijink, I.H.; Hesse, L.; Koo, H.K.; Shaheen, F.; Fouadi, M.; Kuchibhotla, V.; Lambrecht, B.N.; Van Oosterhout, A.; Hackett, T.L.; et al. Characterization of a lung epithelium specific E-cadherin knock-out model: Implications for obstructive lung pathology. *Sci. Rep.* **2018**, *8*, 1. [CrossRef] [PubMed]
14. Bell, R.R.; Nonavinakere, V.K.; Soliman, M.R. Intratracheal exposure of the guinea pig lung to cadmium and/or selenium: A histological evaluation. *Toxicol. Lett.* **2000**, *114*, 101–109. [CrossRef]
15. Cao, X.; Lin, H.; Muskhelishvili, L.; Latendresse, J.; Richter, P.; Heflich, R.H. Tight junction disruption by cadmium in an in vitro human airway tissue model. *Respir. Res.* **2015**, *16*, 30. [CrossRef] [PubMed]
16. Liu, X.; Chen, Z. The pathophysiological role of mitochondrial oxidative stress in lung diseases. *J. Transl. Med.* **2017**, *15*, 207. [CrossRef] [PubMed]
17. Białas, A.J.; Sitarek, P.; Miłkowska-Dymanowska, J.; Piotrowski, W.J.; Górski, P. The Role of Mitochondria and Oxidative/Antioxidative Imbalance in Pathobiology of Chronic Obstructive Pulmonary Disease. *Oxidative Med. Cell. Longev.* **2016**, *2016*, 7808576. [CrossRef] [PubMed]
18. Griffith, B.; Pendyala, S.; Hecker, L.; Lee, P.J.; Natarajan, V.; Thannickal, V.J. NOX enzymes and pulmonary disease. *Antioxid. Redox Signal.* **2009**, *11*, 2505. [CrossRef]
19. Kang, D.; Kim, S.H.; Hamasaki, N. Mitochondrial transcription factor A (TFAM): Roles in maintenance of mtDNA and cellular functions. *Mitochondrion* **2007**, *7*, 39–44. [CrossRef]
20. Kansanen, E.; Kuosmanen, S.M.; Leinonen, H.; Levonen, A.L. The Keap1-Nrf2 pathway: Mechanisms of activation and dysregulation in cancer. *Redox Biol.* **2013**, *1*, 45–49. [CrossRef]
21. Merry, T.L.; Ristow, M. Nuclear factor erythroid-derived 2-like 2 (NFE2L2, Nrf2) mediates exercise-induced mitochondrial biogenesis and the antioxidant response in mice. *J. Physiol.* **2016**, *594*, 5195–5207. [CrossRef]
22. Park, S.H.; Kim, J.H.; Chi, G.Y.; Kim, G.Y.; Chang, Y.C.; Moon, S.K.; Nam, S.W.; Kim, W.J.; Yoo, Y.H.; Choi, Y.H. Induction of apoptosis and autophagy by sodium selenite in A549 human lung carcinoma cells through generation of reactive oxygen species. *Toxicol. Lett.* **2012**, *212*, 252–261. [CrossRef] [PubMed]
23. Montalbano, A.M.; Albano, G.D.; Anzalone, G.; Moscato, M.; Gagliardo, R.; Di Sano, C.; Bonanno, A.; Ruggieri, S.; Cibella, F.; Profita, M. Cytotoxic and genotoxic effects of the flame retardants (PBDE-47, PBDE-99 and PBDE-209) in human bronchial epithelial cells. *Chemosphere* **2020**, *245*, 12. [CrossRef] [PubMed]
24. Kim, A.; Park, S.; Sung, J.H. Cell Viability and Immune Response to Low Concentrations of Nickel and Cadmium: An In Vitro Model. *Int. J. Environ. Res. Public Health* **2020**, *17*, 9218. [CrossRef]
25. Huff, M.O.; Todd, S.L.; Smith, A.L.; Elpers, J.T.; Smith, A.P.; Murphy, R.D.; Bleser-Shartzer, A.S.; Hoerter, J.E.; Radde, B.N.; Klinge, C.M. Arsenite and Cadmium Activate MAPK/ERK via Membrane Estrogen Receptors and G-Protein Coupled Estrogen Receptor Signaling in Human Lung Adenocarcinoma Cells. *Toxicol Sci.* **2016**, *152*, 62–71. [CrossRef] [PubMed]
26. Albano, G.D.; Zhao, J.; Etling, E.B.; Park, S.Y.; Hu, H.; Trudeau, J.B.; Profita, M.; Wenzel, S.E. IL-13 desensitizes β2-adrenergic receptors in human airway epithelial cells through a 15-lipoxygenase/G protein receptor kinase 2 mechanism. *J. Allergy Clin. Immunol.* **2015**, *135*, 1144–1153.e539. [CrossRef]
27. Srinivasan, B.; Kolli, A.R.; Esch, M.B.; Abaci, H.E.; Shuler, M.L.; Hickman, J.J. TEER measurement techniques for in vitro barrier model systems. *J. Lab. Autom.* **2015**, *20*, 107–126. [CrossRef]
28. Shao, J.; White, C.C.; Dabrowski, M.J.; Kavanagh, T.J.; Eckert, M.L.; Gallagher, E.P. The role of mitochondrial and oxidative injury in BDE 47 toxicity to human fetal liver hematopoietic stem cells. *Toxicol. Sci. Off. J. Soc. Toxicol.* **2008**, *101*, 81–90. [CrossRef]
29. Saquib, Q.; Al-Khedhairy, A.A.; Al-Arifi, S.; Dhawan, A.; Musarrat, J. Assessment of methyl thiophanate-Cu (II) induced DNA damage in human lymphocytes. *Toxicol. Vitr. Int. J. Publ. Assoc. BIBRA* **2009**, *23*, 848–854. [CrossRef]
30. Forti, E.; Bulgheroni, A.; Cetin, Y.; Hartung, T.; Jennings, P.; Pfaller, W.; Prieto, P. Characterisation of cadmium chloride induced molecular and functional alterations in airway epithelial cells. *Cell. Physiol. Biochem. Int. J. Exp. Cell. Physiol. Biochem. Pharmacol.* **2010**, *25*, 159–168. [CrossRef]
31. Anzalone, G.; Albano, G.D.; Montalbano, A.M.; Riccobono, L.; Bonanno, A.; Gagliardo, R.; Bucchieri, F.; Marchese, R.; Moscato, M.; Profita, M. IL-17A-associated IKK-α signaling induced TSLP production in epithelial cells of COPD patients. *Exp. Mol. Med.* **2018**, *50*, 1–12. [CrossRef]
32. Leopardi, P.; Cordelli, E.; Villani, P.; Cremona, T.P.; Conti, L.; De Luca, G.; Crebelli, R. Assessment of in vivo genotoxicity of the rodent carcinogen furan: Evaluation of DNA damage and induction of micronuclei in mouse splenocytes. *Mutagenesis* **2010**, *25*, 57–62. [CrossRef]
33. Tanaka, T.; Halicka, D.; Traganos, F.; Darzynkiewicz, Z. Cytometric analysis of DNA damage: Phosphorylation of histone H2AX as a marker of DNA double-strand breaks (DSBs). *Methods Mol. Biol.* **2009**, *523*, 161–168. [CrossRef] [PubMed]

34. Koehler, A. The gender-specific risk to liver toxicity and cancer of flounder (*Platichthys flesus* (L.)) at the German Wadden Sea coast. *Aquat. Toxicol.* **2004**, *70*, 257–276. [CrossRef] [PubMed]
35. Finkel, T.; Holbrook, N.J. Oxidants, oxidative stress and the biology of ageing. *Nature* **2000**, *408*, 239–247. [CrossRef]
36. Prüss-Ustün, A.; Vickers, C.; Haefliger, P.; Bertollini, R. Knowns and unknowns on burden of disease due to chemicals: A systematic review. *Environ. Health A Glob. Access Sci. Source* **2011**, *10*, 9. [CrossRef]
37. Soo-Jin, C.; Jae-Min, O.; Jin-Ho, C. Toxicological effects of inorganic nanoparticles on human lung cancer A549 cells. *J. Inorg. Biochem.* **2009**, *103*, 463–471. [CrossRef]
38. Kim, J.S.; Peters, T.M.; O'Shaughnessy, P.T.; Adamcakova-Dodd, A.; Thorne, P.S. Validation of an in vitro exposure system for toxicity assessment of air-delivered nanomaterials. *Toxicol. Vitr.* **2013**, *27*, 164–173. [CrossRef]
39. Upadhyay, S.; Palmberg, L. Air-Liquid Interface: Relevant in vitro models for investigating air pollutant-induced pulmonary toxicity. *J. Toxicol. Sci.* **2018**, *164*, 21–30. [CrossRef]
40. Skipper, A.; Sims, J.N.; Yedjou, C.G.; Tchounwou, P.B. Cadmium Chloride Induces DNA Damage and Apoptosis of Human Liver Carcinoma Cells via Oxidative Stress. *Int. J. Environ. Res. Public Health* **2016**, *13*, 88. [CrossRef]
41. Lawal, A.O.; Marnewick, J.L.; Ellis, E.M. Heme oxygenase-1 attenuates cadmium-induced mitochondrial-caspase 3- dependent apoptosis in human hepatoma cell line. *BMC Pharmacol. Toxicol.* **2015**, *16*, 41. [CrossRef]
42. Zheng, L.; Jiang, Y.L.; Fei, J.; Cao, P.; Zhuang, J.; Nie, G.; Yang, F.; Dai, X.; Cao, H.; Xing, C.; et al. Cadmium induces cytotoxicity through oxidative stress-mediated apoptosis pathway in duck renal tubular epithelial cells. *Toxicol. Vitr. Int. J. Publ. Assoc. BIBRA* **2019**, *61*, 10. [CrossRef] [PubMed]
43. Yu, X.; Yin, H.; Peng, H.; Lu, G.; Liu, Z.; Dang, Z. OPFRs and BFRs induced A549 cell apoptosis by caspase-dependent mitochondrial pathway. *Chemosphere* **2019**, *221*, 693–702. [CrossRef] [PubMed]
44. Qi, Y.; Li, H.; Zhang, M.; Zhang, T.; Frank, J.; Chen, G. Autophagy in arsenic carcinogenesis. *Exp. Toxicol. Pathol. Off. J. Ges. fur Toxikol. Pathol.* **2014**, *66*, 163–168. [CrossRef]
45. Son, Y.O.; Pratheeshkumar, P.; Roy, R.V.; Hitron, J.A.; Wang, L.; Zhang, Z.; Shi, X. Nrf2/p62 signaling in apoptosis resistance and its role in cadmium-induced carcinogenesis. *J. Biol. Chem.* **2014**, *289*, 28660–28662, Retraction published *J. Biol. Chem.* **2018**, *293*, 15455. [CrossRef]
46. Nyunoya, T.; Mebratu, Y.; Contreras, A.; Delgado, M.; Chand, H.S.; Tesfaigzi, Y. Molecular processes that drive cigarette smoke-induced epithelial cell fate of the lung. *Am. J. Respir. Cell Mol. Biol.* **2014**, *50*, 471–482. [CrossRef]
47. Tran, I.; Ji, C.; Ni, I.; Min, T.; Tang, D.; Vij, N. Role of Cigarette Smoke-Induced Aggresome Formation in Chronic Obstructive Pulmonary Disease-Emphysema Pathogenesis. *Am. J. Respir. Cell Mol. Biol.* **2015**, *53*, 159–173. [CrossRef]
48. de Wit, C.A.; Herzke, D.; Vorkamp, K. Brominated flame retardants in the Arctic environment—Trends and new candidates. *Sci. Total Environ.* **2010**, *408*, 2885. [CrossRef]
49. Pesonen, M.; Vähäkangas, K. Autophagy in exposure to environmental chemicals. *Toxicol. Lett.* **2019**, *305*, 1–9. [CrossRef]
50. Nikoletopoulou, V.; Markaki, M.; Palikaras, K.; Tavernarakis, N. Crosstalk between apoptosis, necrosis and autophagy. *Biochim. Biophys. Acta* **2013**, *1833*, 3448–3459. [CrossRef]
51. Doherty, J.; Baehrecke, E.H. Life, Death and Autophagy. *Nat. Cell Biol.* **2018**, *20*, 1110. [CrossRef]
52. Valverde, M.; Trejo, C.; Rojas, E. Is the capacity of lead acetate and cadmium chloride to induce genotoxic damage due to direct DNA-metal interaction? *Mutagenesis* **2001**, *16*, 265–270. [CrossRef] [PubMed]
53. Oliveira, H.; Monteiro, C.; Pinho, F.; Pinho, S.; Ferreira de Oliveira, J.M.; Santos, C. Cadmium-induced genotoxicity in human osteoblast-like cells. Mutation research. *Genet. Toxicol. Environ. Mutagenesis* **2014**, *775–776*, 38–47. [CrossRef] [PubMed]
54. Rogakou, E.P.; Pilch, D.R.; Orr, A.H.; Ivanova, V.S.; Bonner, W.M. DNA double-stranded breaks induce histone H2AX phosphorylation on serine 139. *J. Biol. Chem.* **1998**, *273*, 5858. [CrossRef] [PubMed]
55. Cleaver, J.E. γH2Ax: Biomarker of damage or functional participant in DNA repair "all that glitters is not gold!". *Photochem. Photobiol.* **2011**, *87*, 1230–1239. [CrossRef] [PubMed]
56. Kopp, B.; Khoury, L.; Audebert, M. Validation of the γH2AX biomarker for genotoxicity assessment: A review. *Arch. Toxicol.* **2019**, *93*, 2103–2114. [CrossRef] [PubMed]
57. Garcia-Canton, C.; Anadón, A.; Meredith, C. γH2AX as a novel endpoint to detect DNA damage: Applications for the assessment of the in vitro genotoxicity of cigarette smoke. *Toxicol. Vitr. Int. J. Assoc. BIBRA* **2012**, *26*, 1075–1086. [CrossRef]
58. Riches, L.C.; Lynch, A.M.; Gooderham, N.J. Early events in the mammalian response to DNA double-strand breaks. *Mutagenesis* **2008**, *23*, 331–339. [CrossRef]
59. Cann, K.L.; Dellaire, G. Heterochromatin and the DNA damage response: The need to relax. *Biochem. Cell Biol.* **2011**, *89*, 45–60. [CrossRef]
60. Xu, Y.; Price, B.D. Chromatin dynamics and the repair of DNA double strand breaks. *Cell Cycle* **2011**, *10*, 261–267. [CrossRef]
61. Navarro-Yepes, J.; Burns, M.; Anandhan, A.; Khalimonchuk, O.; del Razo, L.M.; Quintanilla-Vega, B.; Pappa, A.; Panayiotidis, M.I.; Franco, R. Oxidative stress, redox signaling, and autophagy: Cell death versus survival. *Antioxid. Redox Signal.* **2014**, *21*, 66–85. [CrossRef]
62. Shafique, E.; Choy, W.C.; Liu, Y.; Feng, J.; Cordeiro, B.; Lyra, A.; Arafah, M.; Yassin-Kassab, A.; Zanetti, A.V.; Clements, R.T.; et al. Oxidative stress improves coronary endothelial function through activation of the pro-survival kinase AMPK. *Aging* **2013**, *5*, 515–530. [CrossRef] [PubMed]

63. Sciarretta, S.; Zhai, P.; Shao, D.; Zablocki, D.; Nagarajan, N.; Terada, L.S.; Volpe, M.; Sadoshima, J. Activation of NADPH oxidase 4 in the endoplasmic reticulum promotes cardiomyocyte autophagy and survival during energy stress through the protein kinase RNA-activated-like endoplasmic reticulum kinase/eukaryotic initiation factor 2α/activating transcription factor 4 pathway. *Circ. Res.* **2012**, *113*, 1253–1264. [CrossRef]
64. Dinkova-Kostova, A.T.; Abramov, A.Y. The emerging role of Nrf2 in mitochondrial function. *Free Radic. Biol. Med.* **2015**, *88 Pt B*, 179–188. [CrossRef]
65. Jornayvaz, F.R.; Shulman, G.I. Regulation of mitochondrial biogenesis. *Essays Biochem.* **2010**, *47*, 69–84. [CrossRef] [PubMed]
66. Cloonan, S.M.; Choi, A.M. Mitochondria in lung disease. *J. Clin. Investig.* **2016**, *126*, 809–820. [CrossRef]
67. Tsukita, S.; Tanaka, H.; Tamura, A. The Claudins: From Tight Junctions to Biological Systems. *Trends Biochem. Sci.* **2019**, *44*, 141–152. [CrossRef]
68. Rezaee, F.; Georas, S.N. Breaking barriers. New insights into airway epithelial barrier function in health and disease. *Am. J. Respir. Cell Mol. Biol.* **2014**, *50*, 857–869. [CrossRef]
69. Tam, A.; Wadsworth, S.; Dorscheid, D.; Man, S.F.; Sin, D.D. The airway epithelium: More than just a structural barrier. *Ther. Adv. Respir. Dis.* **2011**, *5*, 255–273. [CrossRef]
70. Li, J.X.H.; Tang, V.W.; Brieher, W.M. Actin protrusions push at apical junctions to maintain E-cadherin adhesion. *Proc. Natl. Acad. Sci. USA* **2020**, *117*, 432–438. [CrossRef]